Paramagnetic ionic plastic crystals containing the octamethylferrocenium cation: counteranion dependence of phase transitions and crystal structures

Mochida, Tomoyuki ; Ishida, Mai ; Tominaga, Takumi ; Takahashi, Kazuyuki ; Sakurai, Takahiro ; Ohta, Hitoshi

(Citation)
Physical Chemistry Chemical Physics,20(5):3019-3028

(Issue Date)
2018-02-07

(Resource Type)
journal article

(Version)
Accepted Manuscript

Phys. Chem. Chem. Phys., **2018**, *20*, 3019–3028.

Paramagnetic ionic plastic crystals containing the octamethylferrocenium cation: counteranion dependence of phase transitions and crystal structures†

Tomoyuki Mochida,*[a] Mai Ishida,[a] Takumi Tominaga,[a] Kazuyuki Takahashi,[a] Takahiro Sakurai[b] and Hitoshi Ohta[cd]

In recent years, ionic plastic crystals have attracted much attention. Many metallocenium salts exhibit plastic phases, but factors affecting their phase transitions are yet to be elucidated. To investigate these factors, we synthesized octamethylferrocenium salts with various counteranions $[Fe(C_5Me_4H)_2]X$ ([**1**]X; X^- = $B(CN)_4^-$, $C(CN)_3^-$, $N(CN)_2^-$, FSA (= $(SO_2F)_2N^-$), $FeCl_4^-$, $GaCl_4^-$ and CPFSA (= $CF_2(SO_2CF_2)_2N^-$)) and elucidated their crystal structures and phase behavior. Correlations between the crystal structures and phase sequences, and the shapes and volumes of the anions are discussed. Except for [**1**][CPFSA], these salts exhibit phase transitions to plastic phases at or above room temperature (T_C = 298–386 K), and the plastic phases exhibit either NaCl- or anti-NiAs-type structures. With the exception of [**1**][CPFSA], which exhibits a structure in which anions and cations are separately stacked to form columns, X-ray crystal structure analyses at 100 K revealed that these structures are composed of alternating arrangements of cations and anions. [**1**][$N(CN)_2$] exhibits a polar crystal structure that undergoes a monotropic phase transition to a centrosymmetric structure. The magnetic susceptibilities of room-temperature plastic crystals [**1**][$GaCl_4$] and [**1**][$FeCl_4$] were investigated; the latter exhibits a small ferromagnetic interaction at low temperatures.

---

[a]*Department of Chemistry, Graduate School of Science, Kobe University, Rokkodai, Nada, Hyogo 657-8501, Japan. E-mail: tmochida@platinum.kobe-u.ac.jp*

[b]*Research Facility Center for Science and Technology, Kobe University, Kobe, Hyogo 657-8501, Japan*

[c]*Department of Physics, Graduate School of Science, Kobe University, Kobe, Hyogo 657-8501, Japan*
[d]*Molecular Photoscience Research Center, Kobe University, Kobe, Hyogo 657-8501, Japan*
†Electronic supplementary information (ESI) available: DSC traces (Fig. S1), powder X-ray diffraction patterns (Fig. S2), ORTEP drawing of the molecular structures (Fig. S3), crystal structures of [**1**][$FeCl_4$] (Fig. S4), and calculated volumes of anions and radius ratios of the salts (Table S1). CCDC 1524593 ([**1**][$B(CN)_4$]), 1541416 ([**1**][$GaCl_4$]), 1541913 ([**1**][$FeCl_4$]), 1536374 ([**1**][$N(CN)_2$], Phase I), 1541409 ([**1**][$N(CN)_2$], Phase II), 1537058 ([**1**][FSA]), 1524657 ([**1**][$C(CN)_3$]), 1524596 ([**1**][CPFSA], Phase I), and 1524597 ([**1**][CPFSA], Phase II). For ESI and crystallographic data in CIF or other electronic format, see DOI:

Introduction

Organic ionic plastic crystals containing various onium cations have attracted much attention over the past few decades because of their possible applications to batteries and capacitors that take advantage of their high ionic conductivities.[1-3] Plastic phases are often exhibited by solids composed of globular molecules that exhibit orientational or rotational disorder. Plastic phases generally have highly symmetric crystal lattices such as cubic or hexagonal.[4] Plastic crystals of neutral organic molecules have small entropies of fusion as a consequence of disorder ($\Delta S < 20$ J K^{-1} mol^{-1}),[4] but the values for ionic plastic crystals can be larger.[1] Such materials often manifest phase transitions from ordered crystalline phases to increasingly disordered structures with increasing temperature.

Salts of sandwich-type organometallic compounds frequently exhibit plastic phases at high temperatures owing to the globular shapes of the cations.[5] For example, [$Fe(C_5H_5)_2$][PF_6] exhibits a plastic phase above 347 K.[5a] We have investigated the phase behavior of various organometallic salts.[6-8] Plastic crystals of ferrocenium salts are expected to be magnetic ionic conductors. Recently, [choline][$FeCl_4$] has been reported to be a magnetic ionic plastic crystal that exhibits antiferromagnetic ordering at low temperatures.[9] Compared with organic plastic crystals, metallocenium salts generally exhibit higher phase transition temperatures to plastic phases;[5,6] hence the search for molecular designs that expand the plastic phase temperature range is important. Previously, the phase transitions in decamethylferrocenium salts [$Fe(C_5Me_5)_2$]X (X^- = BF_4^-, PF_6^-, $CF_3SO_3^-$ (= OTf), $(SO_2CF_3)_2N^-$ (=

Tf_2N)) and the corresponding octamethylferrocenium salts $[Fe(C_5Me_4H)_2]X$ ([**1**]X, Fig. 1a) were systematically investigated.[6] Deca- and octamethylferrocenes are representative polymethyl derivatives of ferrocene. The phase transition temperature to the plastic phase in these salts was found to decrease with increasing anion size, and [**1**]X were found to have lower transition temperatures than $[Fe(C_5Me_5)_2]X$. However, the details of the effect of anion shape and size are still unknown, and the magnetic properties of these compounds have not been well investigated.

To explore the phase transition phenomena and functionalities of metallocenium ionic plastic materials, it is important to elucidate the effect of the anion on crystal structures and phase sequences. In this study, therefore, we synthesized octamethylferrocenium salts ([**1**]X, Fig. 1) with various counteranions, including tetrahedral anions $B(CN)_4^-$, $FeCl_4^-$, and $GaCl_4^-$, bent anions $N(CN)_2^-$ and FSA (= $(SO_2F)_2N^-$), a planar anion $C(CN)_3^-$, and a cyclic anion CPFSA (= $CF_2(S_2O_4CF_2)_2N^-$). With the exception of [**1**][CPFSA], these salts were found to commonly exhibit plastic phases. Firstly, this paper discusses their phase transition temperatures and the structures of their plastic phases. Secondly, the phase sequences of salts that exhibit several solid-solid phase transitions, including the intriguing polar-nonpolar phase transition in [**1**][$N(CN)_2$], are reported. Thirdly, the crystal structure of each salt at low temperature, including structural changes resulting from solid-solid phase transitions, is discussed in relation to anion shape. Finally, the magnetic properties of room-temperature plastic crystals [**1**][$FeCl_4$] and [**1**][$GaCl_4$] are investigated.

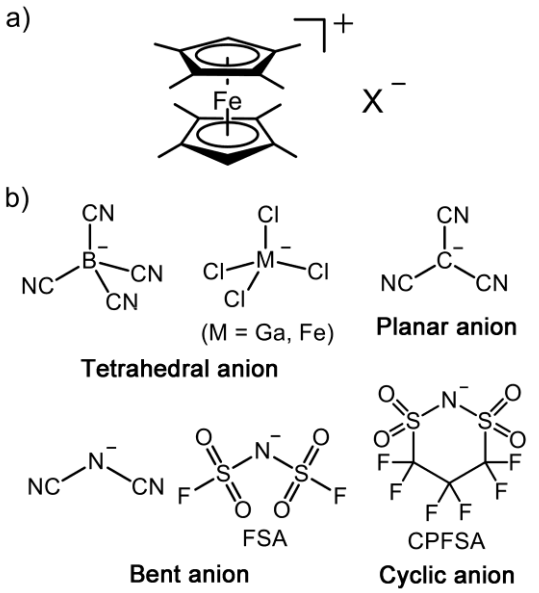

Fig. 1 Structural formulas of (a) octamethylferrocenium salts ([**1**]X), and (b) counteranions (X^-) used in this study.

Results and discussion

Syntheses and properties

The octamethylferrocenium salts were synthesized by the metathesis of [**1**]Cl using alkali metal salts of the corresponding anions. The CN stretching peaks in the IR spectra of [**1**][$C(CN)_3$] (2158 cm^{-1}) and [**1**][$N(CN)_2$] (2124, 2188, 2221 cm^{-1}) were observed at almost the same frequencies as those of [$Fe(C_5Me_5)_2$][$C(CN)_3$] (2162 cm^{-1})[10] and $NaN(CN)_2$, providing evidence that they are monoanionic. The CN stretching peak was absent in [**1**][$B(CN)_4$], which is consistent with the tetrahedral symmetry of this anion.[11]

At the phase transition to a plastic phase, loss of birefringence is observed under a polarization microscope due to the high symmetry of the crystal lattice.[4,5] With the exception of [**1**][CPFSA], polarizing microscope observations revealed that these salts exhibit phase transitions to plastic phases at or above room temperature (T_C = 298–386 K). [**1**][CPFSA] did not exhibit a plastic phase up to its decomposition temperature (T_{dec} = 523 K), which is related to its crystal structure (*vide infra*). [**1**][$C(CN)_3$] melted at around 525 K and immediately decomposed, but the remaining salts did not

melt, rather they directly decomposed at high temperatures.

Phase transitions to plastic phases

The phase transitions in these salts were investigated by differential scanning calorimetry (DSC). The DSC traces are summarized in Fig. S1 (ESI†). Except for [**1**][CPFSA], these salts exhibited phase transitions to plastic phases at temperatures consistent with the polarizing microscope observations. The transition temperatures and transition entropies are summarized in Table 1. The transition temperatures decreased in the order: [**1**][$N(CN)_2$] (386.2 K) > [**1**][FSA] (355.2 K) > [**1**][$C(CN)_3$] (343.3 K) > [**1**][$B(CN)_4$] (312.0 K) > [**1**][$GaCl_4$] (300.8 K) > [**1**][$FeCl_4$] (297.7 K). The transition temperatures were higher for salts containing bent anions ($N(CN)_2$, FSA), and lower for the salts with the MCl_4 anions. To investigate the effect of anion volume, the phase transition temperature of [**1**]X, including data for previously reported salts (X = BF_4, PF_6, OTf, Tf_2N),[6] was plotted versus anion volume (Fig. 2). The anions are smaller than the cation ([**1**]$^+$: V = 325.7 Å^3). This figure indicates that the phase transition temperature tends to decrease with increasing anion volume. This tendency seems to be reasonable because interionic Coulomb interactions are expected to decrease with increasing anion volume. The transition temperature of [**1**][$B(CN)_4$] is higher than those of [**1**][MCl_4] despite its larger anion volume, which may be ascribed to a greater deviation in anion shape from spherical. Salts of anions with lower symmetry than tetrahedral or octahedral tend to exhibit higher transition temperatures, although [**1**][OTf] (T_C = 288.6 K)[6] has an exceptionally low transition temperature, being the lowest among the octamethylferrocenium salts investigated. There appears to be no correlation between molecular shape and the transition entropy (ΔS) or the sum of the solid-solid phase transition entropies (ΔS_{total}).

For comparison with [**1**][$FeCl_4$], DSC measurements were performed on [$Fe(C_5Me_5)_2$][$FeCl_4$]. This salt exhibited a phase transition to its plastic phase at 363.3 K (ΔS = 25.5 J mol^{-1} K^{-1}), at a much higher temperature than [**1**][$FeCl_4$] (297.7 K), and their transition entropies were comparable. This result supports the observation that [**1**]X exhibit plastic phases at lower temperatures than [$Fe(C_5Me_5)_2$]X, as observed for salts with other anions (X = BF_4, PF_6, OTf, Tf_2N).[6]

Table 1 Phase transition temperatures (T_C) and transition entropies (ΔS) to plastic phases in [**1**]X.

	T_C (K)	ΔS (J mol^{-1} K^{-1})	ΔS_{total} (J mol^{-1} K^{-1})[a]
[**1**][$B(CN)_4$]	312.0	45.2	
[**1**][$C(CN)_3$]	343.3	76.9	
[**1**][$N(CN)_2$]	385.6	27.8	65.6
[**1**][FSA]	355.2	34.4	35.7
[**1**][$GaCl_4$]	300.8	41.3	
[**1**][$FeCl_4$]	297.7	26.8	
[$Fe(C_5Me_5)_2$][$FeCl_4$]	363.3	25.5	
[**1**][BF_4][b]	409.0	27.7	
[**1**][PF_6][b]	349.1	39.8	43.2
[**1**][OTf][b]	288.6	35.8	
[**1**][Tf_2N][b]	318.6	54.2	55.9
[$Fe(C_5Me_5)_2$][Tf_2N][b]	398.1	46.9	47.9

[a]Sum of solid-solid phase transition entropies for salts that exhibit several phase transitions in the solid state. [b]Data from ref. 6.

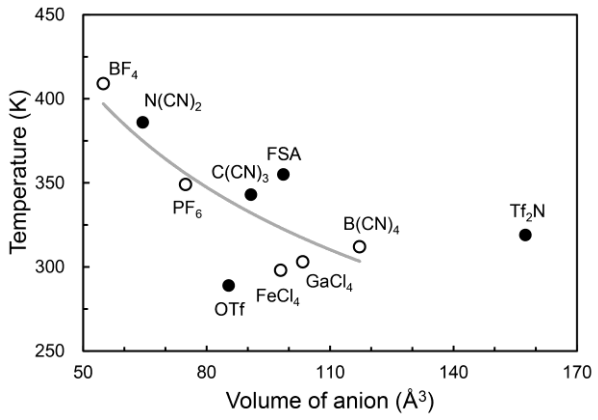

Fig. 2 Phase transition temperature to a plastic phase in [**1**]X plotted versus anion volume. Tetrahedral and octahedral anions are indicated by open circles (○), and other anions by filled circles (●). The gray line is a best-fit curve for salts excluding Tf_2N.

Crystal structures of the plastic phases

The structures of the plastic phases of [**1**]X (X = $B(CN)_4$, $C(CN)_3$, $FeCl_4$) were investigated by powder

X-ray diffraction (PXRD) measurements (Fig. S2; ESI†), which reveal that [**1**][$B(CN)_4$] and [**1**][$C(CN)_3$] have anti-NiAs-type structures, whereas [**1**][$FeCl_4$] has a NaCl-type structure. Each structure has a coordination number of six. Only a few plastic crystals having the anti-NiAs-type structure are known; these are NiAs structures with larger cations than anions.[3a] The van der Waals (vdW) radii of the ions estimated from DFT calculations are 4.22 Å for $[\mathbf{1}]^+$ and 2.73–3.03 Å for the anions; hence the interionic distances are estimated to be 7.01–7.25 Å, which are comparable (slightly shorter by approximately 0.4 Å) to the interionic distances determined from the lattice constants (6.57–6.87 Å) (Table 2).

According to the radius ratio rule in ionic crystals, coordination numbers are expected to be six for cation–anion radius ratios (ρ) of 0.41–0.73, and eight for ratios greater than 0.73.[12] Based on the van der Waals radii of the ions (above), the radius ratios ($\rho = r_{anion}/r_{cation}$) for [**1**]X (X = $B(CN)_4$, $C(CN)_3$, $FeCl_4$) were estimated to be 0.66–0.72 (Table 2); consequently their six-coordination structures are in agreement with the radius ratio rule. The PXRD patterns of [**1**][$N(CN)_2$] and [**1**][FSA] could not be obtained because of their high transition temperatures, but their radius ratios (0.59 and 0.68, respectively) also predict a coordination number of six for each structure.

Table 2 Structure types, lattice constants, interionic distances, and radius ratios (calculated values) of salts [**1**]X

Compound	Temperature (K)[a]	Structure Type	Lattice constants (Å)	Interionic distances (exp., Å)	(calc., Å)[b]	Radius ratio (r^-/r^+, calc.)[b]
[**1**][$B(CN)_4$]	333	anti-NiAs	$a = b = 8.98$, $c = 13.49$	6.87	7.25	0.72
[**1**][$C(CN)_3$]	363	anti-NiAs	$a = b = 8.81$, $c = 12.46$	6.57	7.01	0.66
[**1**][$FeCl_4$]	313	NaCl	$a = b = c = 13.41(6)$	6.71	7.18	0.68

[a]Temperature at which the measurement was conducted. [b]Based on the van der Waals radii estimated by DFT calculations.

Phase sequences of [1][N(CN)$_2$], [1][FSA], and [1][CPFSA]

The salts with polar anions [**1**][$N(CN)_2$] and [**1**][FSA] exhibited several solid-solid phase transitions. [**1**][CPFSA], which does not exhibit a plastic phase, underwent several phase transitions, while the other salts exhibited only phase transitions to plastic phases.

[**1**][$N(CN)_2$] underwent solid phase transitions at 318.9 K (phase I to II; ΔS = 12.3 J mol^{-1} K^{-1}) and

336.7 K (phase II to III; ΔS = 25.5 J mol^{-1} K^{-1}), followed by a transition to a plastic phase at 385.6 K (ΔS = 27.8 J mol^{-1} K^{-1}) (Fig. 3a). The DSC trace of this salt is shown in Fig. 4. Intriguingly, the phase transition from phase I to II is a transition from a polar crystal structure having a ferroelectric anionic arrangement to a centrosymmetric structure (*vide infra*). This is a monotropic phase transition, which is probably due to the centrosymmetric structure of phase II being electrostatically favored over the polar structure of phase I. Both phase I and II exhibit no disorder; hence phase III might be an anion-disordered phase when the phase transitions of other metallocenium salts are considered.[6,7]

[**1**][FSA] underwent phase transitions at 340.9 K (phase I to II: ΔS = 1.3 J mol^{-1} K^{-1}) and 355.3 K (phase II to plastic: ΔS = 34.4 J mol^{-1} K^{-1}) (Fig. 3b). Although FSA and Tf_2N anions frequently exhibit disorder in the solid state,[2a,6,7] only one of two crystallographically independent anions was disordered in phase I (*vide infra*). The transition from phase I to II might be related to the disordering of the other anion. No phase transition was observed below room temperature, which is in contrast to the phase transitions observed for [Co(C_5H_5)$_2$][FSA] and [**1**][Tf_2N] that are accompanied by anion ordering.[6,7]

[**1**][CPFSA] underwent phase transitions at 255.1 K (phase I to II: ΔS = 9.9 J mol^{-1} K^{-1}) and 316.3 K (phase II to III: ΔS = 67.3 J mol^{-1} K^{-1}) (Fig. 3c). The molecular arrangement changed slightly at the first phase transition (*vide infra*). Phase III underwent a further phase transition to phase IV at 275.5 K (ΔS = 15.4 J mol^{-1} K^{-1}) upon cooling. Therefore, this salt did not return to phase II once it had transformed into phase III, although phase IV is a thermodynamically metastable phase.

Our previous study showed that [Fe(C_5Me_5)$_2$]X (X = BF_4, Tf_2N) and [**1**]X (X = PF_6, Tf_2N) undergo successive phase transitions from ordered phases to anion-disordered phases, and then to plastic phases.[6] In the present salts, however, such a gradual disordering tendency was not clearly observed, although the phase transitions in [**1**][FSA] and [**1**][$N(CN)_2$] are possibly accompanied by order-disorder of the anion.

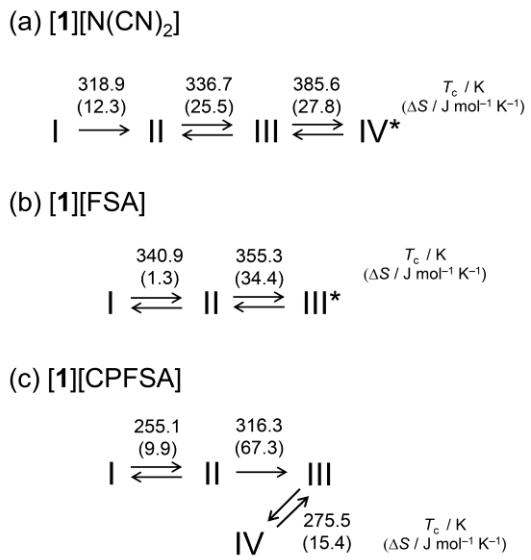

Fig. 3 Phase sequences of (a) [**1**][$N(CN)_2$], (b) [**1**][FSA], and (c) [**1**][CPFSA]. The phase transition temperatures and transition entropies (in parentheses) are also shown. The asterisks indicate plastic phases.

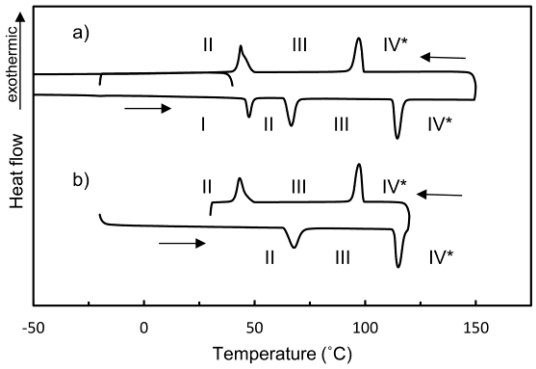

Fig. 4 DSC trace of [**1**][$N(CN)_2$] measured at 10 K min^{-1} (a: 1st cycle, b: 2nd cycle).

General features of crystal structures

The crystal structures of these salts in phase I were determined at 100 K. [**1**][MCl_4] (M = Fe, Ga) were isomorphous. [**1**][$N(CN)_2$] and [**1**][FSA], containing polar anions, exhibited polar crystal structures, while the remaining salts had centrosymmetric crystal structures. ORTEP drawings of the molecular structures are shown in Fig. S3 (ESI†).

Concerning the molecular arrangements within the crystals, with the exception of [**1**][CPFSA], the cations and anions were alternately arranged in these salts. In these crystals, the number of anions

surrounding a given cation, and *vice versa*, was six. The estimated radius ratios (r_{anion}/r_{cation}) for these salts, based on the calculated vdW radii, were 0.59–0.72. Therefore, although the molecular shapes are not spherical, the radius ratio rule for ionic crystals seems to hold, which predicts coordination numbers of six for radius ratios between 0.41–0.73.[12] In contrast, [**1**][CPFSA] has a segregated-stack structure, in which cations and anions are separately stacked to form columns in the crystal.

Based on this and previous studies, $C(CN)_3$ and CPFSA were found to give both alternately arranged structures and segregated-stack structures depending on the cation. The $C(CN)_3$ anion is planar and can form intermolecular π–π interactions; [**1**][$C(CN)_3$] exhibits the alternately arranged structure through cation–anion π–π interactions, although [$Ru(C_5H_5)(C_6H_6)$][$C(CN)_3$][8] exhibits a segregated-stack structure through cation-cation and anion-anion π–π interactions. The CPFSA anion has a globular shape and is likely to form an alternating arrangement and exhibit plastic phases, as observed in [$Co(C_5H_5)_2$][CPFSA] and [NR_4][CPFSA].[7,13] However, [**1**][CPFSA] exhibited a segregated-stack structure with no plastic phase. The absence of plastic phases in segregated-stack salts is in accord with our previous observation for [$Ru(C_5H_5)(C_6H_6)$][$C(CN)_3$] and [$Co(C_5H_5)_2$][$(C_nF_{2n+1}SO_2)_2N$].[7,8] It seems reasonable that segregated-stack salts are unable to transform into plastic phases with isotropic structures because large structural changes are required.

Concerning the orientations of the cation, except for [**1**][$B(CN)_4$], the C_5 axes of the ferrocenyl moieties are aligned uniaxially in these crystals. This tendency has also been observed in [**1**]X with other anions (X^- = BF_4^-, PF_6^-, Tf_2N^-).[6] Since the ferrocenium cation has the largest *g*-value component along the C_5 axis, crystals of these salts exhibit uniaxial magnetic anisotropy. This feature may be useful for controlling magnetic properties.[14] In contrast, [**1**][$B(CN)_4$] exhibited an in-plane distribution of the C_5 axes of the cations. In [**1**][$N(CN)_2$], phase II has a smaller magnetic anisotropy than phase I.

In ferrocenium salts with cyano-containing anions, the N atom of the anion is often located near the Fe atom of the cation (Fe···N distance: ~4.1–4.7 Å). This close arrangement causes cation-anion electrostatic interactions, although these distances are greater than the vdW contact distance.[15] In [**1**]X (X = $B(CN)_4$, $C(CN)_3$, $N(CN)_2$), two CN groups are located close to the Fe atom (Fe···N distance: 4.5–4.8 Å). In [**1**][FSA] and [**1**][CPFSA], one N atom is located close to the Fe atom (Fe···N distance: 4.3

Å) to form an ion pair. In octamethylferrocenium salts, short contacts are frequently observed between the ring hydrogen atoms of the cation and the negatively charged atoms of the anion.[16] This type of contact is observed in salts other than [**1**][$C(CN)_3$], and include CH···N (X = $B(CN)_4$, $N(CN)_2$, CPFSA), CH···O (X = FSA), and CH···Cl contacts (X = $GaCl_4$) that are 0.1–0.3 Å shorter than the corresponding vdW contact distances.

The following sections describe details of the crystal structures of the salts, with reference to the shapes of the anions. The structural changes in [**1**][$N(CN)_2$] and [**1**][CPFSA] during their transitions from phase I to II are also discussed.

Crystal structures of [1][$B(CN)_4$] and [1][MCl_4] (M = Ga, Fe)

[**1**][$B(CN)_4$] and [**1**][MCl_4] (M = Ga, Fe), having tetrahedral anions, exhibit simple alternating arrangements of cations and anions in their unit cells.

The packing diagram of [**1**][$B(CN)_4$] is shown in Fig. 5. This salt crystallized in the space group $I4_1/acd$, with one crystallographically independent cation and anion (Z = 16). There are two kinds of cations in the unit cell, whose C_5 axes are oriented almost perpendicular to each other in the *ab* plane. The packing diagram of [**1**][$GaCl_4$] (space group $P\bar{1}$, Z = 4) is shown in Fig. 6. [**1**][$FeCl_4$] and [**1**][$GaCl_4$] are isomorphous, and have comparable lattice volumes (2217 $Å^3$; Fig. S4, ESI†). There are two pairs of crystallographically independent cations and anions in the structure of [**1**][$GaCl_4$]. The C_5 axes of the ferrocenyl moieties are approximately aligned along the [011] direction. There are several short intermolecular Cl–π and Cl–HC cation-anion contacts, which are 0.15–0.2 Å shorter than the sum of the vdW radii. The corresponding decamethylferrocenium salt [$Fe(C_5Me_5)_2$][$FeCl_4$] (space group $P\bar{1}$, Z = 2)[17] has a different unit cell, but its molecular arrangement is somewhat similar to that of **[1]**[$FeCl_4$].

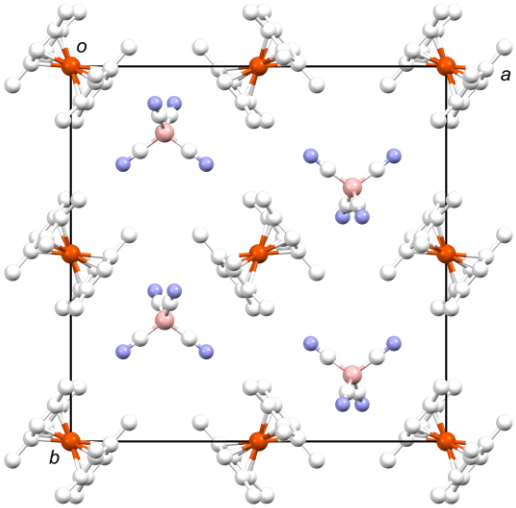

Fig. 5 Packing diagram of [**1**][B(CN)$_4$] ($I4_1/acd$, $Z = 16$) at 100 K. Only molecules in the *ab* plane are included for clarity.

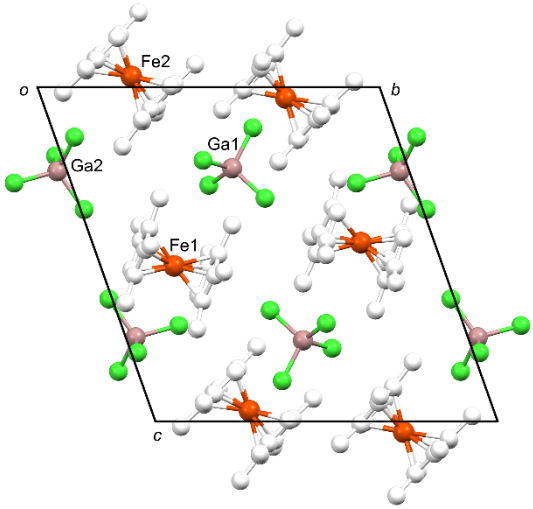

Fig. 6 Packing diagram of [**1**][GaCl$_4$] (space group $P\bar{1}$, $Z = 4$) at 100 K.

Crystal structures of [1][N(CN)$_2$] and [1][FSA]

[**1**][N(CN)$_2$] and [**1**][FSA], which contain polar anions, crystallized in polar space groups in phase I. It is intriguing that the former salt monotropically transforms into a centrosymmetric structure in phase II.

The packing diagram of [**1**][N(CN)$_2$] in phase I at 100 K is shown in Fig. 7a. This salt crystallized in the space group *Pn*, with one crystallographically independent cation and anion ($Z = 2$). The dipole moments of the anions were aligned approximately along the *a*-axis in a ferroelectric manner. The C_5

axis of the ferrocenyl moiety is approximately oriented along the *a*-axis. The packing diagram of phase II is shown in Fig. 7b. The transition from phase I to phase II at 319 K is monotropic, hence the structure was determined at 100 K on a sample that had been heated to above the transition temperature. The unit cell volume of phase II is twice of that of phase I, having a centrosymmetric space group $P2_1/c$ ($Z = 4$). Accordingly, the anions are arranged such that their dipole moments cancel each other, as seen in Fig. 7b. Two centrosymmetric cations and one anion are crystallographically independent. The torsion angle between the cyclopentadienyl rings in the ferrocenyl moieties (C–Cp^1–Cp^2–C, where Cp^1 and Cp^2 are the centroids of the rings) changes from 11° in phase I to 36° in phase II. The C_5 axes of the cations in phase II are oriented in several directions; consequently phase II exhibits a smaller magnetic anisotropy than phase I.

The packing diagram of [**1**][FSA] is shown in Fig. 8. This salt crystallized in the space group $Pca2_1$, with two crystallographically independent cation and anion ($Z = 8$). The C_5 axes of the cations are aligned along the *b*-axis. The two independent anions are arranged in a nearly centrosymmetric manner; one exhibits a two-fold disorder of the central N atom and the terminal -CFO_2 groups, as is often observed in salts of FSA or Tf_2N (Fig. S3d; ESI†).[2a,6] This partial disorder is ascribable to the less-distorted arrangements of cations around disordered anions than those around ordered anions. A similar partial disordering of anions is also seen in $[Co(C_5H_5)_2][(CF_3CH_2SO_2)_2N]$.[7] The packing arrangement of this salt resembles that of [**1**][Tf_2N], but the anion in [**1**][Tf_2N] is disordered in the room-temperature phase and ordered after a low-temperature phase transition.[6] In [**1**][FSA], the central N atom of the anion is close enough to the Fe atom (N···Fe distances: 4.4 or 4.7 Å for Fe1, and 4.5 Å for Fe2) to form ion pairs.

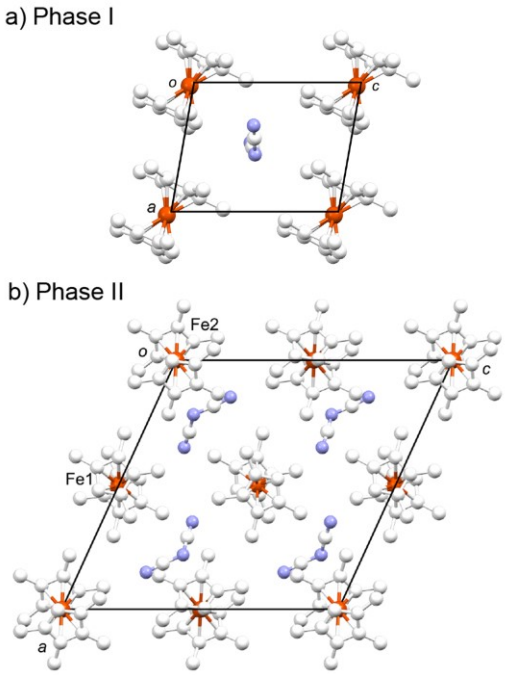

Fig. 7 Packing diagrams of [**1**][N(CN)$_2$] in: (a) phase I (*P*n, *Z* = 2), and (b) phase II (*P*2$_1$/c, *Z* = 4) at 100 K.

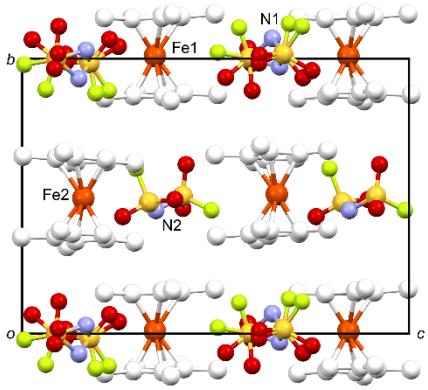

Fig. 8 Packing diagram of [**1**][FSA] at 100 K (*P*ca2$_1$, *Z* = 8).

Crystal structures of [1][C(CN)$_3$] and [1][CPFSA]

The structure of [**1**][C(CN)$_3$], which contains a planar anion, consists of alternately π–π stacked cations and anions. In contrast, [**1**][CPFSA] has a segregated-stack structure, in which the anions and cations are separately stacked to form columns.

The packing diagram of [**1**][C(CN)$_3$] is shown in Fig. 9. This salt crystallized in the space group *P*bca, with one crystallographically independent cation and anion (*Z* = 8). The cations and anions are

alternately arranged, although the planes of the anions and cyclopentadienyl rings of the cations are canted toward each other. The C_5 axes of the cations are aligned along the *b*-axis of the crystal. This structure is very different to that of $[Fe(C_5Me_5)_2][C(CN)_3]$ (space group *P*ma2) that has a complicated arrangement of cations,[10] although the alternating cation-anion arrangement is similar.

The crystal structures of [**1**][CPFSA] in phases I and II were determined at 100 K and 293 K, respectively. Their packing diagrams are shown in Figs. 10a and 10b; the cations and anions are separately stacked to form segregated columns. In both phases, the space group of [**1**][CPFSA] is $P2_1/n$, with two crystallographically independent cation and anion ($Z = 4$). The N atoms of the anions are located close to the Fe atoms to form ion pairs (N···Fe distance: 4.3–4.4 Å). The C_5 axes of the cations are approximately aligned along the *b*-axis. In phase II of [**1**][CPFSA], the intermolecular distances between the centroids of the cyclopentadienyl rings of the cations are 4.10 and 4.82 Å (Fig. 10a). However, column dimers are formed in phase I, with corresponding distances of 3.48 Å and 4.88 Å (Fig. 10b), the former being markedly shorter than the corresponding distance in phase II. The torsion angle between the cyclopentadienyl rings in the ferrocenyl moiety changes during phase transition, from 1° in phase I to 11° in phase II (Fig. S3f; ESI†).

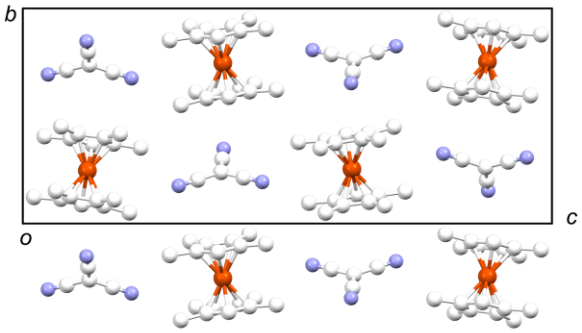

Fig. 9 Packing diagram of [**1**][$C(CN)_3$] (*P*bca, $Z = 8$) at 100 K. Only molecules in the *bc* plane are included for clarity.

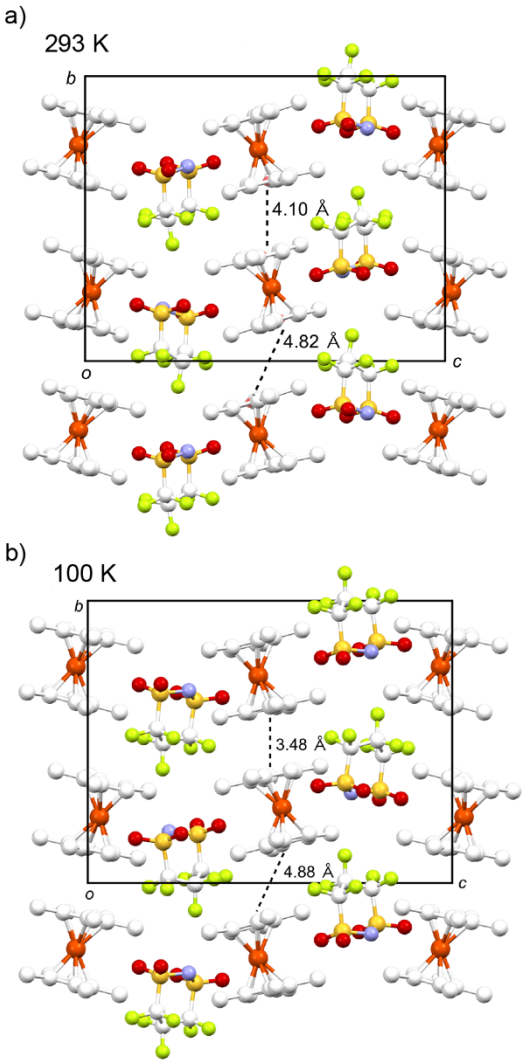

Fig. 10 Packing diagrams of [**1**][$C_3F_6NO_4S_2$] ($P2_1/n$, Z = 4) at (a) 293 K and (b) 100 K. The dotted lines indicate the intermolecular distances between the centroids of the cyclopentadienyl rings.

Magnetic susceptibilities of [1][$GaCl_4$] and [1][$FeCl_4$]

[**1**][$GaCl_4$] and [**1**][$FeCl_4$], having the lowest phase-transition temperatures to plastic phases among the salts investigated, are regarded as room-temperature magnetic plastic crystals. The temperature dependences of their magnetic susceptibilities (χT values) are shown in Fig. 11. These salts exhibited simple paramagnetic behavior. The χT value of [**1**][$GaCl_4$], containing the diamagnetic anion, is 0.66 emu K mol^{-1} at 273 K, which corresponds to the magnetic susceptibility of the ferrocenium cation.[17] The magnetic moment decreases only slightly at low temperatures. On the other hand, the χT value for

[**1**][$FeCl_4$] at 273 K is 5.15 emu K mol^{-1}, which is equal to the sum of the magnetic susceptibilities of the ferrocenium cation (0.7 emu K mol^{-1}) and $FeCl_4$ (S = 5/2, 4.375 emu K mol^{-1}). At temperatures below 20 K, the magnetic moment increases, which indicates the presence of a small ferromagnetic interaction. Fitting of this temperature dependence to the Curie-Weiss law ($\chi = C/(T-\theta)$) gave $\theta = +0.9$ K. This observation is intriguing because onium salts with $FeCl_4$ usually exhibit very small antiferromagnetic interactions.[18] In [**1**][$FeCl_4$], there are no direct cation-cation and anion-anion contacts, hence the short Cl–π and Cl–HC contacts between the cation and anion (*vide supra*) might provide pathways for ferromagnetic (or ferrimagnetic) interactions. Another possibly related phenomenon is the ferromagnetic interaction in [$Fe(C_5Me_4H)_2$][TCNE] resulting from the spin-polarization mechanism.[19] Complicated magnetic behavior, such as successive magnetic ordering, has been reported for related ferrocenium salts [$FeCp_2$][FeX_4] (X = Cl, Br).[20]

The magnetic susceptibilities of these salts changed only slightly during phase transitions from their plastic to ordered phases; the magnetic susceptibilities increased by 0.03 and 0.15 emu K mol^{-1}, respectively (Fig. 11, insets), and exhibited almost no magnetic-field dependence. This result indicates the absence of magnetic orientation phenomena during the phase transition. We previously reported that magnetic field orientations occur during the liquid–solid phase transitions of ionic liquids containing ferrocenium cations owing to their magnetic anisotropies,[11] which were accompanied by marked increases in magnetic susceptibility. It seems reasonable that magnetic field orientations are less likely to occur during the solid–solid phase transitions.

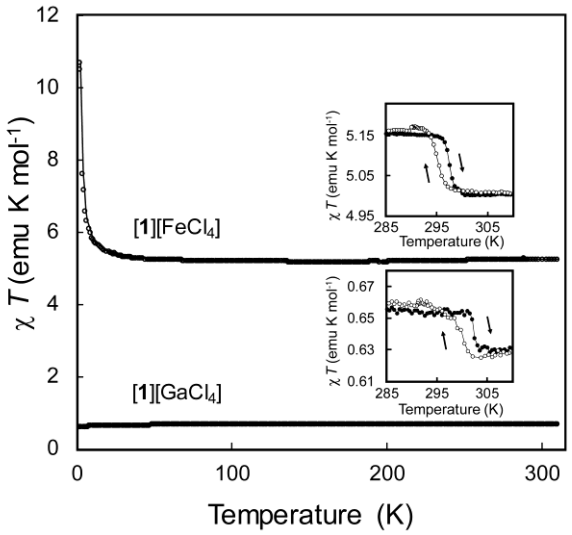

Fig. 11 Temperature dependences of the magnetic susceptibilities (χT) of [**1**][$FeCl_4$] and [**1**][$GaCl_4$] measured under 0.1 T. The insets show enlarged views around the phase I to plastic phase transition temperatures measured under 1 T.

Conclusions

As part of our continuing investigations into the development of functional organometallic soft materials, we synthesized octamethylferrocenium salts with anions of various shapes and volumes. These salts exhibit phase transitions to plastic phases at or above room temperature. These transition temperatures were observed to decrease with increasing anion volume, and symmetrical anions tended to exhibit higher transition temperatures than centrosymmetric anions. The structures of the plastic phases follow the radius ratio rule for ionic crystals and adopt NaCl- or anti-NiAs-type structures. The cations and anions are also arranged in an alternating fashion in these salts in their low temperature phases. In the crystals of octamethylferrocenium salts, the C_5 axes of the ferrocenium moieties tend to be uniaxially oriented in the low temperature phases.

As an exception, the CPFSA salt did not exhibit a plastic phase. This salt has a segregated-stack structure, where the anions and cations are separately stacked to form columns. The absence of plastic phases in segregated-stack salts is in accordance with our previous observations of related salts. $N(CN)_2$ and CPFSA anions were found to give both types of salts, having alternately arranged

structures or segregated-stack structures, depending on the cation.

The salts containing $GaCl_4$ and $FeCl_4$ are room-temperature paramagnetic plastic crystals, of which the latter exhibits a very small ferromagnetic interaction at low temperatures. These salts do not exhibit magnetic field orientations during phase transitions from the plastic to crystal phases. The salts with polar anions (FSA and $N(CN)_2$) crystallize in polar space groups and exhibit several phase transitions. It is intriguing that the $N(CN)_2$ salt, having a ferroelectric arrangement of anions, undergoes a monotropic phase transition to a centrosymmetric structure at high temperature. These findings suggest that the use of polar anions may lead to the construction of ferroelectric materials.

The findings obtained in this study are useful for the design of magnetic plastic crystal materials and magnetic dielectric materials. Detailed physical properties of these and related salts will be investigated in these laboratories.

Experimental

General

$[Fe(C_5Me_4H)_2][PF_6]$ ([**1**][PF_6]) was synthesized following the literature procedure.[21] $[Fe(C_5Me_5)_2][PF_6]$ was synthesized by an analogous method.[22] Other chemicals were commercially available. DSC measurements were performed using a TA Q100 differential scanning calorimeter at a scan rate of 10 K min^{-1}. Infrared spectra were acquired via attenuated total reflectance (ATR, diamond) using a Thermo Nicolet Avatar 360 FT-IR spectrometer. Powder XRD measurements at room temperature were performed using a Rigaku SmartLab diffractometer with CuKα radiation (λ = 1.5418 Å). Variable temperature powder X-ray diffraction experiments were performed using a Bruker APEX II Ultra CCD diffractometer with MoKα radiation (λ = 0.71073 Å). Indexing of powder XRD data was performed manually. Magnetic susceptibilities were measured using a Quantum Design MPMS-XL instrument under 0.1–5 T. Van der Waals volumes of the cations and anions were estimated by DFT calculations.[6] Calculations were performed at the B3LYP/LanL2DZ level of theory using the Spartan'16 software (Wavefunction Inc.), and the ionic radii were tentatively calculated assuming spheres of the same volumes as the ions. Calculated volumes of anions and radius ratios of the salts

are summarized in Table S1 (ESI†).

Synthesis

[Fe($C_5Me_4H)_2$]Cl ([1]Cl). Dowex anion exchange resin (Dowex 1X8-100) was suspended in methanol and allowed to stand for 1 h. The resin was then packed into a column and washed with a methanol solution of tetrabutylammonium chloride (50 mM, 50 mL) and methanol (100 mL). A solution of [**1**][PF_6] (64 mg, 0.14 mmol) in a mixture of methanol (15 mL) and acetone (3 mL) was then eluted through the column using methanol as the eluent. Evaporation of the column-collected solution afforded [**1**]Cl as a pale yellow oil in quantitative yield, which was used for subsequent anion exchange reactions, as described below.

[Fe($C_5Me_4H)_2$][$B(CN)_4$] ([1][$B(CN)_4$]). K[$B(CN)_4$] (31 mg, 0.20 mmol) was added to a solution of [**1**]Cl (60 mg, 0.18 mmol) in dichloromethane (4 mL), followed by stirring for 1 h. The solution was dried over magnesium sulfate, filtered, and the solvent evaporated at reduced pressure. The residue was dissolved in dichloromethane-diethyl ether, and the solution was cooled slowly from room temperature to –40 °C. The precipitated crystals were collected by filtration and dried under vacuum to give the desired product (yield 29 mg, 40%). Anal. Calcd. for $C_{22}H_{26}BFeN_4$: C, 63.96; H, 6.34; N, 13.56. Found: C, 63.68; H, 6.33; N, 13.43. IR (cm^{-1}): 1462, 1386, 1026, 965, 932, 891, 839.

[Fe($C_5Me_4H)_2$][$C(CN)_3$] ([1][$C(CN)_3$]). This salt was prepared as described for [**1**][$B(CN)_4$], except that Na[$C(CN)_3$] was used instead of K[$B(CN)_4$]. The product was recrystallized twice from dichloromethane–hexane (Yield 22%). Anal. Calcd. for $C_{22}H_{26}FeN_3$: C, 68.05; H, 6.75 ; N, 10.82. Found: C, 67.95; H, 6.66; N, 10.80. IR (cm^{-1}): 2158 (CN), 1454, 1387, 1026, 859, 557.

[Fe($C_5Me_4H)_2$][$N(CN)_2$] ([1][$N(CN)_2$]). Na[$N(CN)_2$] (31 mg, 0.34 mmol) was added to a solution of [**1**]Cl (88.4 mg, 0.27 mmol) in dichloromethane (4 mL) followed by stirring for 1 h. After addition of water, the mixture was extracted three times with dichloromethane. The organic layer was combined, dried over magnesium sulfate, and filtered. The solvent was evaporated at reduced pressure, and the residue was recrystallized from dichloromethane–hexane (yield 18 mg, 18%). Anal. Calcd. for $C_{20}H_{26}FeN_3$: C, 65.94; H, 7.19; N, 11.53. Found: C, 65.84; H, 6.95; N, 11.60. IR (cm^{-1}): 2221 (CN),

2188 (CN), 2124 (CN), 1450, 1385, 1376, 1297, 1023.

[Fe($C_5Me_4H)_2$][FSA] ([1][FSA]). This salt was prepared as described for [**1**][$C(CN)_3$], except that K[FSA] was used instead of Na[$N(CN)_2$] (yield 47%). Anal. Calcd. for $C_{22}H_{26}F_2FeO_4S_2N$: C, 45.19; H, 5.48; N 2.93. Found: C, 45.39; H, 5.63; N, 2.90. IR (cm^{-1}): 1480, 1450, 1420, 1214, 1175 (SO), 1100, 1026, 864, 823, 689.

[Fe($C_5Me_4H)_2$][$FeCl_4$] ([1][$FeCl_4$]). $FeCl_3$ (58 mg, 0.36 mmol) was slowly added to a solution of [**1**]Cl (115 mg, 0.34 mmol) in dichloromethane (4 mL) with stirring. After 30 min, the solution was filtered, and the filtrate was evaporated at reduced pressure. The product was recrystallized from acetone–diethyl ether (yield 66 mg, 58%). Anal. Calcd. for $C_{22}H_{26}Cl_4Fe$: C, 43.60; H, 5.28; N, 0.00. Found: C, 43.71; H, 5.39; N, 0.02. IR (cm^{-1}): 1471, 1450, 1383, 1023, 865 (FeCl).

[Fe($C_5Me_4H)_2$][$GaCl_4$] ([1][$GaCl_4$]). A solution of [**1**]Cl (88.0 mg, 0.26 mmol) in ethanol (4 mL) was added to a solution of $GaCl_3$ (81 mg, 0.46 mmol) in concentrated hydrochloric acid (0.5 mL). After stirring for 2 h, the product was collected by filtration, and was washed with ethanol and diethyl ether. The product was purified by recrystallization from acetone–diethyl ether (54 mg, 40%). Anal. Calcd. for $C_{22}H_{26}Cl_4Ga$: C, 42.41; H, 5.14; N 0.00. Found: C, 42.16; H, 5.12; N, 0.00. IR (cm^{-1}): 1478, 1447, 1417, 1384, 1365, 1022, 864, 689, 564.

[Fe($C_5Me_4H)_2$][$C_3F_6NO_4S_2$] ([1][$C_3F_6NO_4S_2$]). This salt was prepared as described for [**1**][$B(CN)_4$], except that Li[$C_3F_6NO_4S_2$] was used instead of K[$B(CN)_4$]. The product was recrystallized twice from dichloromethane–hexane (yield 12%). Anal. Calcd. for $C_{21}H_{26}F_6FeNO_4S_2$: C, 42.72; H, 4.44; N, 2.37. Found: C, 42.72; H, 4.22; N, 2.50. IR (cm^{-1}): 1352 (CF), 1155 (SO), 1087 (SO), 1037 (SO), 994, 795, 602.

X-ray structure determinations

Single crystals of [**1**][$C(CN)_3$], [**1**][FSA], and [**1**][CPFSA] for use in X-ray crystallography were obtained by recrystallization from dichloromethane-hexane, while those of [**1**][$N(CN)_2$] were recrystallized from dichloromethane-diethyl ether. Single crystals of [**1**][$B(CN)_4$] and [**1**][MCl_4] (M = Ga, Fe) were grown by vapor diffusion of diethyl ether into acetonitrile and acetone solutions,

respectively. XRD data were collected using a Bruker APEX II Ultra CCD diffractometer with MoKα radiation (λ = 0.71073 Å) at 100 K. Measurements on [**1**][$C_3F_6NO_4S_2$] were also carried out at 296 K. The measurement of phase II of [**1**][$N(CN)_2$] was carried out at 100 K using a sample that had been heated to 323 K followed by cooling. The rates of heating and cooling were 1 K min^{-1}. The structures were determined by direct methods using SHELXL.[23] The crystallographic parameters are listed in Tables 3 and 4. The structure of [**1**][$N(CN)_2$] (phase II) was refined as a two-component twin, whereas those of [**1**][$GaCl_4$] and [**1**][$FeCl_4$] were refined as merohedral twins. ORTEP-3 for Windows[24] and Mercury[25] were used to produce molecular graphics.

Table 3 Crystallographic parameters

	[**1**][$B(CN)_4$]	[**1**][$C(CN)_3$]	[**1**][$N(CN)_2$]		[**1**][FSA]
			Phase I	Phase II	
Empirical formula	$C_{22}H_{26}BFeN_4$	$C_{22}H_{26}FeN_3$	$C_{20}H_{26}FeN_3$		$C_{18}H_{26}F_2FeNO_4S_2$
Formula weight	413.13	388.31	364.29		478.38
Crystal system	tetragonal	orthorhombic	monoclinic	monoclinic	orthorhombic
Space group	*I*4$_1$/*acd*	*Pbca*	*Pn*	*P*2$_1$/*c*	*Pca*2$_1$
a [Å]	19.357(2)	12.203(2)	7.3025(18)	16.360(15)	19.718(3)
b [Å]	19.357(2)	11.584(2)	13.588(3)	7.436(7)	12.134(2)
c [Å]	23.627(3)	28.223(5)	9.390(2)	16.530(15)	17.156(3)
β [°]	90	90	100.099(3)	114.611(11)	90
V [Å^3]	8853.1(19)	3989.6(12)	917.3(4)	1828(3)	4104.7(12)
Z	16	8	2	4	8
ρ_{calcd} [g cm^{-3}]	1.240	1.293	1.319	1.323	1.548
F(000)	3472	1640	386	772	1992
Temperature [K]	100	100	100	100	100
Reflns collected	24192	20250	5070	8073	23029
Independent reflns	2550	4244	3051	4127	9225
Parameters	133	244	226	229	597
R(int)	0.0228	0.0310	0.0185	0.0487	0.0384
R_1[a], R_w[b] ($I > 2\sigma$)	0.0314. 0.0899	0.0378, 0.0925	0.0190, 0.0497	0.0528, 0.1233	0.0798, 0.1897
R_1[a], R_w[b] (all data)	0.0361, 0.0960	0.0404, 0.0940	0.0192, 0.0496	0.0968, 0.1445	0.0846, 0.1934
Goodness of fit	1.074	1.265	1.073	1.051	1.097
$\Delta\rho_{max,min}$ [e Å^{-3}]	0.295, –0.311	0.451, –0.261	0.537, –0.162	0.381, –0.557	1.280, –2.046

[a] $R_1 = \Sigma||F_o| - |F_c|| / \Sigma|F_o|$. [b] $R_w = [\Sigma w (F_o^2 - F_c^2)^2 / \Sigma w (F_o^2)^2]^{1/2}$

Table 4 Crystallographic parameters

	[**1**][$GaCl_4$]	[**1**][$FeCl_4$]	[**1**][CPFSA]	
			Phase I	Phase II
Empirical formula	$C_{18}H_{26}Cl_4FeGa$	$C_{18}H_{26}Cl_4Fe_2$	$C_{21}H_{26}F_6FeNO_4S_2$	
Formula weight	509.76	495.89	590.40	
Crystal system	triclinic	triclinic	monoclinic	monoclinic
Space group	*P*-1	*P*–1	$P2_1/n$	$P2_1/n$
a [Å]	9.0583(13)	9.064(5)	8.917(2)	8.9842(4)
b [Å]	15.893(2)	15.866(9)	14.441(4)	14.8711(7)
c [Å]	16.379(2)	16.381(10)	19.074(5)	19.1820(8)
α [°]	70.496(2)	70.651(7)	90	90
β [°]	89.297(2)	89.289(8)	102.995(3)	102.4470(10)
γ [°]	86.103(2)	86.092(7)	90	90
V [Å^3]	2217.4(5)	2217(2)	2393.3(11)	2502.57(19)
Z	4	4	4	4
ρ_{calcd} [g cm^{-3}]	1.527	1.486	1.639	1.567
F(000)	1036	1016	1212	1212
Temperature [K]	100	100	100	296
Reflns collected	9282	9230	12869	14056
Independent reflns	9282	8145	5051	5505
Parameters	451	451	324	324
R(int)	0.0000	0.0828	0.0279	0.0157
$R_1{}^a$, $R_w{}^b$ ($I > 2\sigma$)	0.0374, 0.1031	0.0988, 0.2648	0.0260, 0.0723	0.0430, 0.1261
$R_1{}^a$, $R_w{}^b$ (all data)	0.0430, 0.1064	0.1067, 0.2694	0.0271, 0.0734	0.0484, 0.1202
Goodness of fit	1.044	1.159	1.047	1.039
$\Delta\rho_{max,min}$ [e Å^{-3}]	1.361, –0.716	3.325, –1.438	0.500, –0.386	0.764, –0.608

$^aR_1 = \Sigma||F_o| - |F_c|| / \Sigma|F_o|$. $^bR_w = [\Sigma w (F_o^2 - F_c^2)^2 / \Sigma w (F_o^2)^2]^{1/2}$

Acknowledgments

This work was financially supported by KAKENHI (grant number 16H04132) from the Japan Society for the Promotion of Science (JSPS). We are grateful to Hironori Kimata (Kobe University) for the SQUID measurement of [**1**][$GaCl_4$] and Dr. Yusuke Funasako (Tokyo University of Science, Yamaguchi) for his help with X-ray crystallography. We also thank the anonymous reviewers for their valuable comments.

References

1. *(a)* D. R. MacFarlane, J. Huang and M. Forsyth, *Nature*, 1999, **402**, 792–794; *(b)* J. M. Pringle, *Phys. Chem. Chem. Phys*., 2013, **15**, 1339–1351; *(c)* Y. Abu-Lebdeh, P.-J. Alarco and M. Armand, *Angew. Chem., Int. Ed.*, 2003, **42**, 4499–4501; *(d)* J. Luo, A. H. Jensen, N. R. Brooks, J. Sniekers, M. Knipper, D. Aili, Q. Li, B. Vanroy, M. Wübbenhorst, F. Yan, L. V. Meervelt, Z. Shao, J. Fang, Z.-H. Luo, D. E. De Vos, K. Binnemans and J. Fransaer, *Energy Environ. Sci.*, 2015, **8**, 1276–1291; *(e)* M. Lee, U. H. Choi, S. Wi, C. Slebodnick, R. H. Colby and H. W. Gibson, *J. Mater. Chem.*, 2011**, 21**, 12280–12287.

2. *(a)* W. A. Henderson, M. Herstedt, V. G. Young, Jr., S. Passerini, H. C. De Long and P. C. Trulove, *Inorg. Chem.*, 2006, **45**, 1412–1414; *(b)* W. A. Henderson, V. G. Young, Jr., S. Passerini, P. C. Trulove and H. C. De Long, *Chem. Mat.*, 2006, **18**, 934–938; *(c)* Y. Lauw, T. Rüther, M. D. Horne, K. S. Wallwork, B. W. Skelton, I. C. Madsen and T. Rodopoulos, *Cryst. Growth Des.*, 2012, **12**, 2803–2813; *(d)* H. Ishida, T. Iwachido, N. Hayama, R. Ikeda, M. Terashima and D. Nakamura, *Z. Naturforsch*., 1989, **44A**, 741–746.

3. *(a)* K. Matsumoto, U. Harinaga, R. Tanaka, A. Koyama, R. Hagiwara and K. Tsunashima, *Phys. Chem. Chem. Phys*., 2014, **16**, 23616–23626; *(b)* T. Enomoto, S. Kanematsu, K. Tsunashima, K. Matsumoto and R. Hagiwara, *Phys. Chem. Chem. Phys.*, 2011, **13**, 12536–12544; (*c)* Z. -B. Zhou and H. Matsumoto, *Electrochem. Commun.*, 2007, **9**, 1017–1022; *(d)* T. Hayasaki, S. Hirakawa and H. Honda, *Bull. Chem. Soc. Jpn.*, 2013, **86**, 993–1001.

4. *(a)* J. Timmermans, *J. Phys. Chem. Solids*, 1961, **18**, 1–8; *(b)* J. Sherwood, The Plastically Crystalline State: Orientationally Disordered Crystals, Wiley, Chichester, UK, 1979.

5. *(a)* R. J. Webb, M. D. Lowery, Y. Shiomi, M. Sorai, R. J. Wittebort and D. N. Hendrickson, *Inorg. Chem.*, 1992, **31**, 5211–5219; *(b)* D. Braga, F. Paganelli, E, Tagliavini, S. Casolari, G. Cojazzi and F. Grepioni, *Organometallics*, 1999, **18**, 4191–4196; *(c)* H. Schottenberger, K. Wurst, U. J. Griesser, R. K. R. Jetti, G. Laus, R. H. Herber and I. Nowik, *J. Am. Chem. Soc*., 2005, **127**, 6795–6801.

6. T. Mochida, Y. Funasako, M. Ishida, S. Saruta, T. Kosone and T. Kitazawa, *Chem. Eur. J.*, 2016, **22**, 15725–15732.

7. T. Mochida, Y. Funasako, T. Inagaki, M. J. Li, K. Asahara and D. Kuwahara, *Chem. Eur. J.*, 2013, **19**, 6257–6264.

8. T. Tominaga, T. Ueda and T. Mochida, *Phys. Chem. Chem. Phys.*, 2017, **19**, 4352–4359.

9. I. de Pedro, A. García-Saiz, J. A. González, I. Ruiz de Larramendi, T. Rojo, C. Afonso, S. Simeonov, J. C. Waerenborgh, J. A. Blanco, B. Ramajo and J. Rodríguez, *Phys. Chem. Chem. Phys.*, 2013, **15**, 12724–12733.

10. D. A. Dixon, J. C. Calabrese and J. S. Miller, *J. Am. Chem. Soc.*, 1986, **108**, 2582–2588.

11. E. Bernhardt, G. Henkel and H. Willner, *Z. Anorg. Allg. Chem.*, 2000, **626**, 560–568.

12. P. Atkins, T. Overton, J. Rourke, M. Weller, F. Armstrong, Shriver and Atkins' Inorganic

Chemistry, Oxford University Press, Oxford, 2010.
13. M. Moriya, T. Watanabe, W. Sakamoto and T. Yogo, *RSC Adv.*, 2012, **2**, 8502–8507.
14. Y. Funasako, T. Mochida, T. Inagaki, T. Sakurai, H. Ohta, K. Furukara and T. Nakamura, *Chem. Commun.*, 2011, **47**, 4475–4477.
15. T. Mochida, Y. Funasako, E. Nagabuchi and H. Mori, *Cryst. Growth Des.*, 2014, **14**, 1459–1466.
16. Y. Funasako, T. Inagaki, T. Mochida, T. Sakurai, H. Ohta, K. Furukawa and T. Nakamura, *Dalton Trans.*, 2013, **42**, 8317–8327.
17. CSD refcode HIGDOQ, S. Zuercher, V. Gramlich and A. Togni, CSD communication, 1999.
18. Z. Warnke, E. Styczeń, D. Wyrzykowski, A. Sikorski, J. Kłak and J. Mroziński, *Struct. Chem.*, 2010, **21**, 285–289.
19. J. S. Miller, D. T. Glatzhofer, D. M. O'Hare, W. M. Reiff, A. Chakraborty and A. J. Epstein, *Inorg. Chem.*, 1989, **28**, 2930–2939.
20. (*a*) W. M. Reiff, J. H. Zhang and C. P. Landee, *Solid State Commun*., 1993, **88**, 427–430; (*b*) W.M. Reiff, J. -H. Zhang and J. S. Miller, *Hyperfine Int*., 1994, **94**, 2105–2110; (*c*) K. Padmakumar, T. Pradeep, J. Ensling, P. Gütlich and P. T. Manoharan, *Indian J. Chem.*, 2003, **42A**, 2359–2370.
21. A. N. Nesmeyanov, R. B. Materikova, I. R. Lyatifov, T. K. Kurbanov and N. S. Kochetkova, *J. Organomet. Chem.*, 1978, **145**, 241–243.
22. J. M. Forward, D. M. P. Mingos and A. V. Powell, *J. Organomet. Chem.*, 1994, **465**, 251–258.
23. G. M. Sheldrick, *Acta Crystallogr.*, 2008, **A64**, 112−122.
24. L. J. Farrugia, *J. Appl. Crystallogr.*, 1999, **32**, 837−838.
25. C. F. Macrae, I. J. Bruno, J. A. Chisholm, P. R. Edgington, P. McCabe, E. Pidcock, L. Rodriguez-Monge, R. Taylor, J. van de Streek and P. A. Wood, *J. Appl. Crystallogr.*, 2008, **41**, 466−470.

TOC

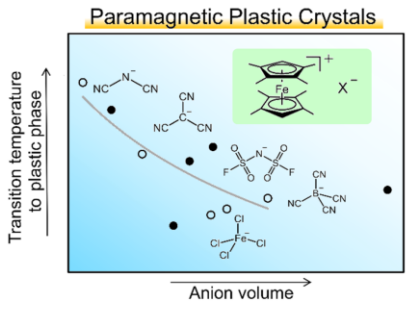

Octamethylferrocenium salts with various anions exhibit paramagnetic plastic phases at or above room temperature.

Supporting Information

Paramagnetic ionic plastic crystals containing the octamethylferrocenium cation: counteranion dependence of phase transitions and crystal structures

Tomoyuki Mochida,*[a] Mai Ishida,[a] Takumi Tominaga,[a] Kazuyuki Takahashi,[a] Takahiro Sakurai[b] and Hitoshi Ohta[cd]

[a]*Department of Chemistry, Graduate School of Science, Kobe University, Rokkodai, Nada, Hyogo 657-8501, Japan. E-mail: tmochida@platinum.kobe-u.ac.jp*

[b]*Research Facility Center for Science and Technology, Kobe University, Kobe, Hyogo 657-8501, Japan*

[c]*Department of Physics, Graduate School of Science, Kobe University, Kobe, Hyogo 657-8501, Japan*

[d]*Molecular Photoscience Research Center, Kobe University, Kobe, Hyogo 657-8501, Japan*

a) [**1**][$B(CN)_4$] b) [**1**][$C(CN)_3$]

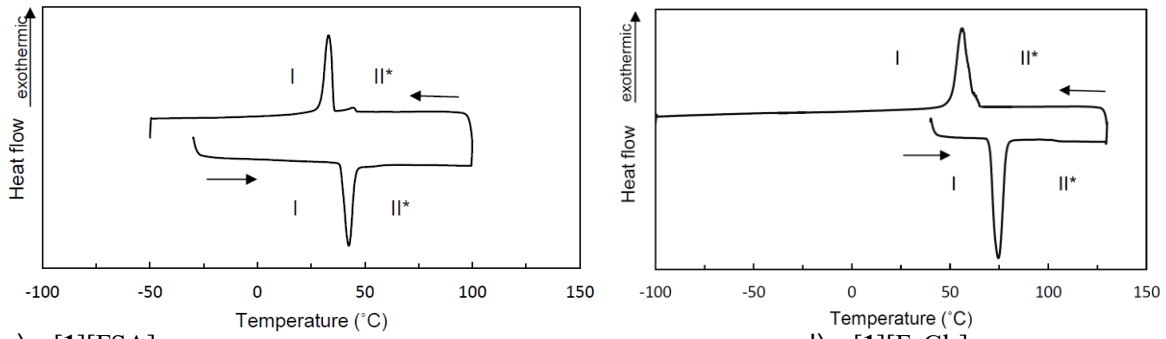

c) [**1**][FSA] d) [**1**][$FeCl_4$]

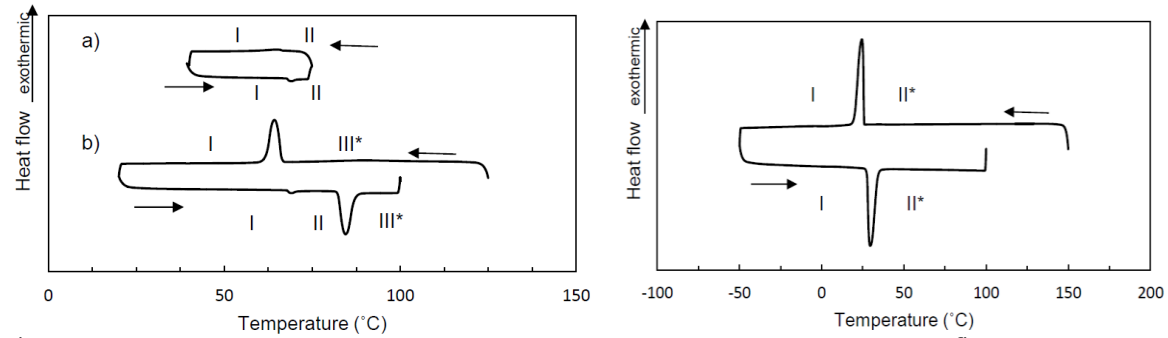

e) [**1**][$GaCl_4$] f) [**1**][CPFSA]

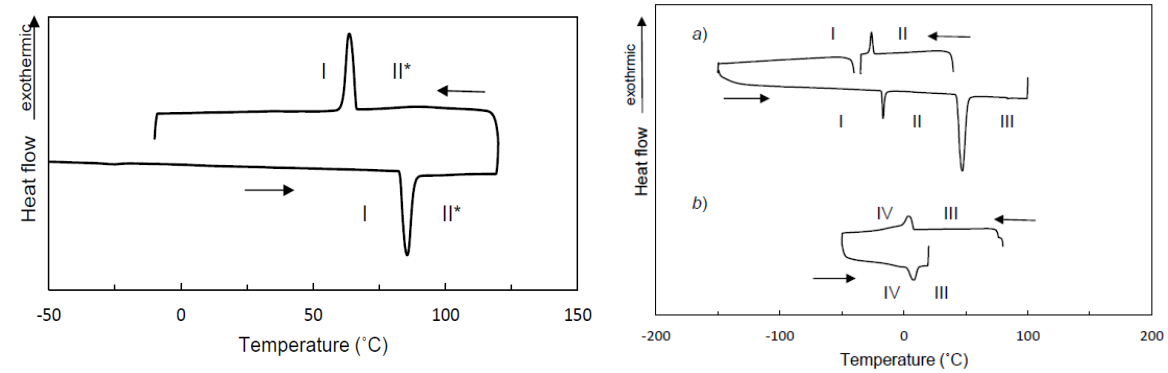

Fig. S1 DSC traces of the salts; *a* and *b* denote the 1st and 2nd cycles, respectively. Asterisks indicate plastic phases.

a) [**1**][$B(CN)_4$]

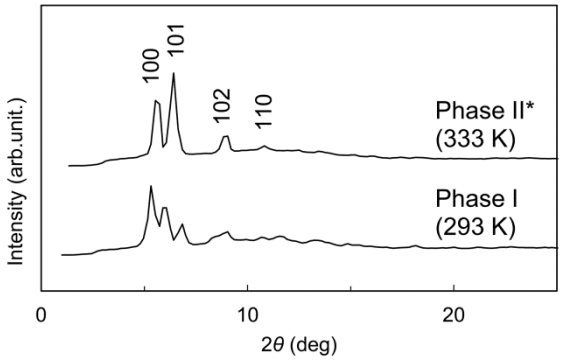

b) [**1**][$C(CN)_3$]

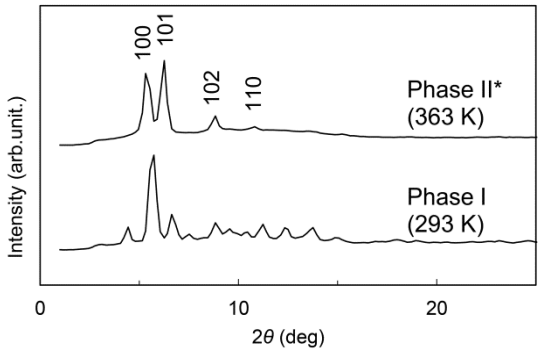

c) [**1**][$FeCl_4$]

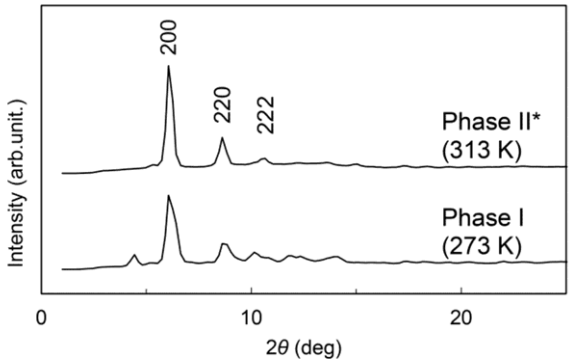

Fig. S2 Powder X-ray diffraction patterns of (a) [**1**][$B(CN)_4$], (b) [**1**][$C(CN)_3$], and (c) [**1**][$FeCl_4$] (MoKα radiation, $\lambda = 0.71073$ Å).

a) [**1**][$B(CN)_4$] b) [**1**][$C(CN)_3$]

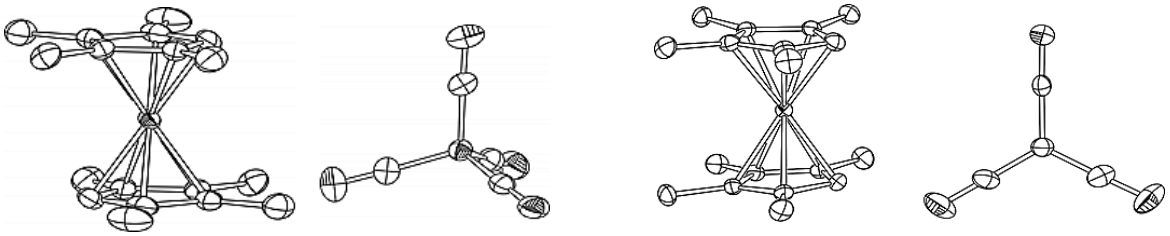

c) [**1**][$N(CN)_2$]

Phase I Phase II

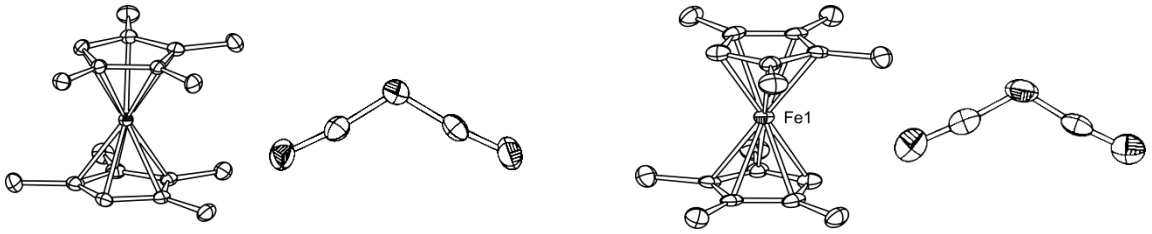

d) [**1**][FSA] e) [**1**][$GaCl_4$]

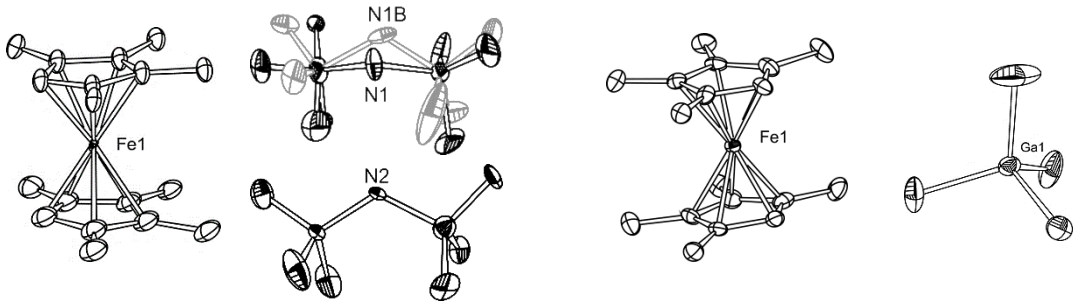

f) [**1**][CPFSA]

293 K 100 K

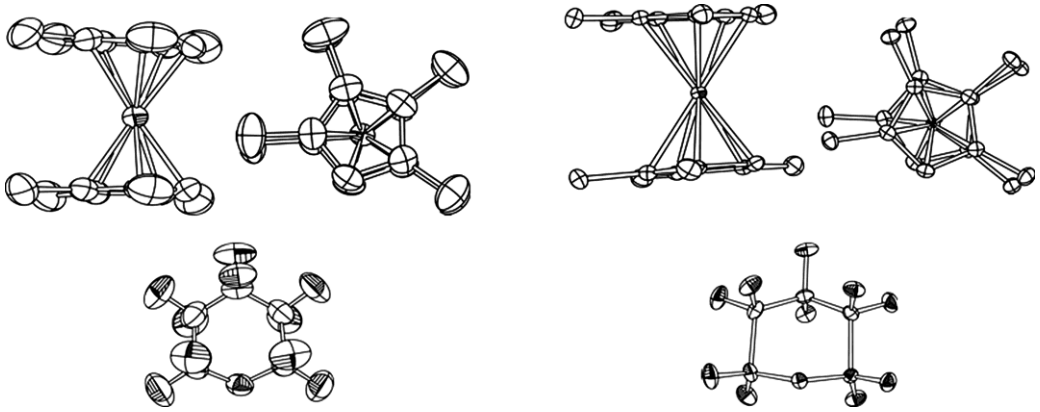

Fig. S3 ORTEP drawings of the cations and anions in each salt at 100 K. Hydrogen atoms have been omitted for clarity. Only one of the two crystallographically independent cations or anions are shown for [**1**][$N(CN)_2$] (phase II), [**1**][FSA], and [**1**][$GaCl_4$], since the molecules are almost identical.

a) b)

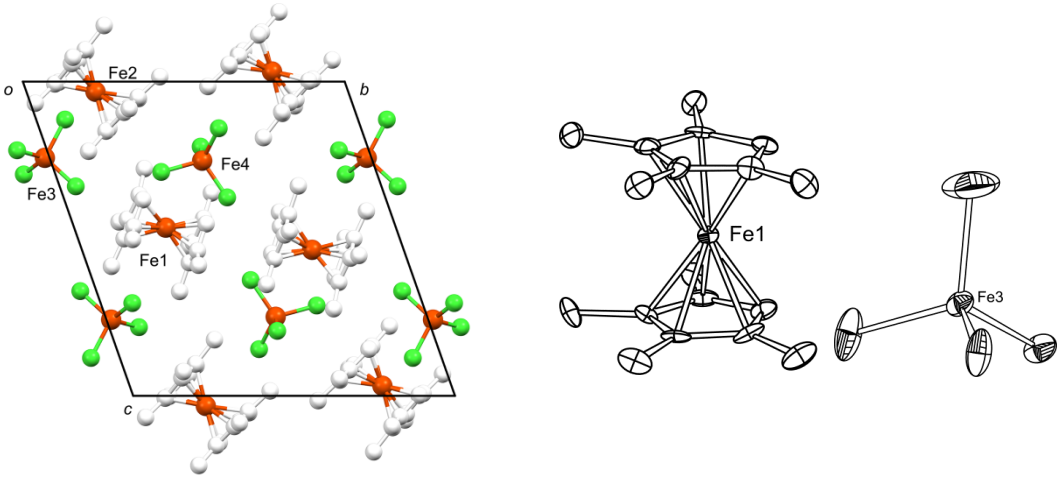

Fig. S4 (a) Packing diagram, and (b) ORTEP drawing of [**1**][$FeCl_4$] at 100 K. In (b), only molecules containing Fe1 and Fe3 are shown, because those containing Fe2 and Fe4 are structurally almost identical. Hydrogen atoms have been omitted for clarity.

Table S1 Anion volumes, van der Waals radii of anions, and radius ratios of the salts estimated from DFT calculations

	Anion volume (Å^3)	van der Waals radius (Å)	Radius ratio (r^-/r^+)
[**1**][BF_4][a]	54.9	2.36	0.559
[**1**][$N(CN)_2$]	64.5	2.49	0.590
[**1**][PF_6][a]	74.9	2.61	0.620
[**1**][OTf][a]	85.4	2.73	0.647
[**1**][$C(CN)_3$]	90.8	2.79	0.660
[**1**][$FeCl_4$]	98.0	2.86	0.677
[**1**][FSA]	98.7	2.87	0.679
[**1**][$GaCl_4$]	103.4	2.91	0.689
[**1**][$B(CN)_4$]	117.2	3.03	0.719
[**1**][Tf_2N][a]	157.5	3.35	0.794
[**1**][CPFSA]	162.3	3.38	0.801

[a]Mochida, *et al*., *Chem. Eur. J*., **22**, 15725 (2016).